

AN ANALYSIS OF ROCK FAILURE AROUND A DEEP LONGWALL USING MICROSEISMICS

Keith A. Heasley, *Section Chief, Geotechnical Engineering*

John L. Ellenberger, *Research Geophysicist*

Paul W. Jeran, *Research Geologist*

National Institute for Occupational Safety and Health

Pittsburgh Research Laboratory

Pittsburgh, Pennsylvania USA

ABSTRACT

In this paper, a state-of-the-art, three-dimensional, full waveform, microseismic system was used to analyze the rock failure around a deep (> 750 m (2500 ft) of cover) bump-prone longwall panel. The microseismic system consisted of both underground and surface geophones coupled through radio telemetry and a fiber-optic network to produce pseudo real-time detection and location of seismic events surrounding the coal seam. This was the first microseismic installation of this scope at a U.S. coal mine, and the system was intended to help determine the exact strata mechanics associated with the redistribution of stress and the associated gob formation at one of the U.S.'s deepest longwall mines. Overall, 5,000 calibrated seismic events were recorded during the mining of one panel, including a Richter magnitude 4.2 event which occurred inside of the array. Analysis of these events provides a number of notable insights into the rock mass behavior. For instance, the longwall panel was widened during the retreat process, and the mining-induced seismicity shows a distinctly different behavior between the start of the panel, the mining of the narrow part of the panel and the mining of the wider part of the panel. Also, in itself, the acquisition of the M_L 4.2 event was a major milestone in geomechanical and bump research. This is the first time that such an event has been recorded with this detail and accuracy at a bump-prone coal mine in the U.S. The analysis of this single event has set distinct new limits on the relationship between mining seismicity and coal bumps.

INTRODUCTION

In recent years, microseismic systems have been used in coal mines in Australia and the United States to gain a better understanding of the ground failures and rock mechanics involved with longwall mining (1-5). These microseismic systems "listen" to the rock and determine the timing and location of the failure of the rock strata surrounding the longwall panel. The recent hardware and software advances in microseismic systems have allowed this geophysical monitoring technique to provide practical geomechanical measurements at operating mines (6). The results from these measurements have been insights into longwall geomechanics that are somewhat outside of previous strata mechanics understanding. The microseismic events and associated rock failure have mostly been recorded from well in front of the longwall face, with a noticeable lack of seismic activity coming from the gob area. The seismic events

have been distributed fairly evenly above and below the seam and the predominant fracture mechanism has been shear failure (as determined from focal analysis and numerical modeling (2)).

The primary objective of the field work presented in this paper was to examine the strata failure behavior of a deep, bump-prone longwall mine using a three-dimensional seismic monitoring system. By analyzing the observed rock failure, we hope to increase our knowledge of the processes governing caving of the massive main roof, the compaction and load acquisition of the gob, the failure of the floor, and the stress redistribution in the coalbed and surrounding strata. The application of this knowledge will enable better mine designs in the future in order to mitigate dangerous bump occurrences and unexpected failures of the massive overburden.

GEOLOGY

This research was conducted at a longwall coal mine in Utah, situated in the area of the Book Cliffs and the eastern Wasatch Plateau in the northwest corner of the Colorado Plateau. In this area, the coal seams are located in the Blackhawk Formation of the Mesa Verde Group (figure 1) (7). The study mine is primarily in the Castlegate 'D' Seam; however, over part of the study area, the underlying Kenilworth Seam and the Castlegate 'D' Seam coalesce and the mine operates in the joined seam. The resultant coalbed at the mine ranges from 2.4 to 6.0 m (8 to 20 ft) in thickness with an extraction thickness of 2.4 to 3.0 m (8 to 10 ft). The geology immediately above and below the seam consists of thinner (<3 m (< 10 ft)) layers of delta deposited siltstones, mudstones, shales, sandstones, and coal. Above the coal bearing portion of the Blackhawk Formation, approximately 150-180 m (500-600 ft) of braided stream deposits with numerous lenticular sandstone channels occur (8). These braided and lenticular deposits make up the immediate and main roofs of the mine.

Unconformably overlying the Blackhawk Formation is the Castlegate Sandstone. The Castlegate is a massive, cliff forming sandstone that is 120 to 180 m (400 to 600 ft) thick with the lower 90 m (300 ft) being more compact and massive than the upper portion of the unit (8). In the mine area, the Castlegate Sandstone lies approximately 200 m (680 ft) above the "D" seam (8). Overlying the Castlegate is the Price River Formation, consisting primarily of sandstone with interbedded conglomerates and sandstones. The Price River Formation is also about 180 m (600 ft) in thickness. The

uppermost rocks exposed at the site are lacustrine deposits of the North Horn Formation, consisting of interbedded claystones, mudstones, limestones, siltstones, and sandstones. Overall, the overburden at this mine reaches up to 900 m (3,000 ft) thick (figure 2).

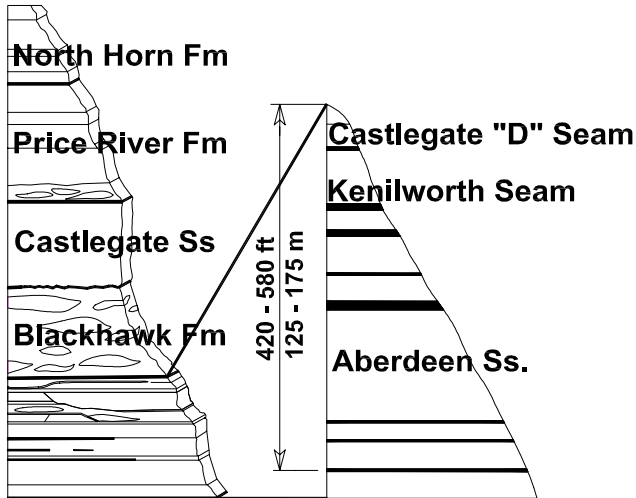


Figure 1. Generalized stratigraphy

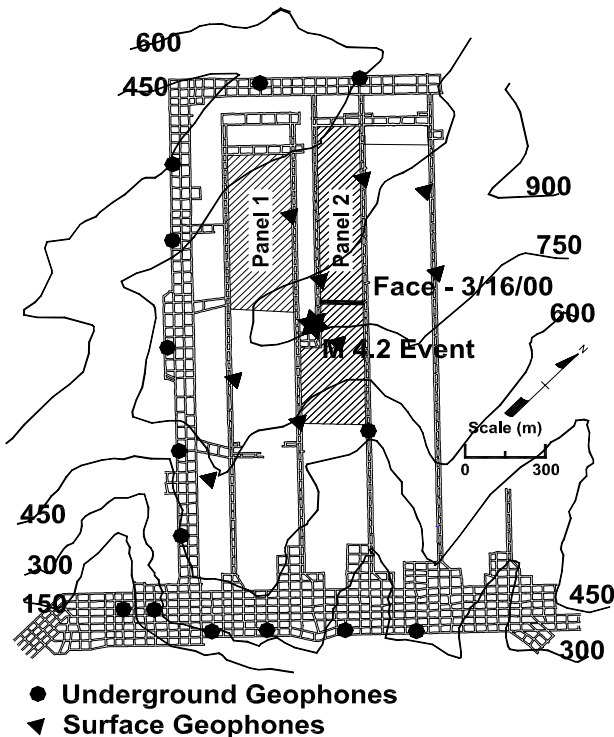


Figure 2. Plan view showing mine layout, overburden, geophone arrays, and the location of the M 4.2 event

MICROSEISMIC SYSTEM

The microseismic monitoring array consisted of 23 geophones deployed both underground in the mine entries and on the surface above the mine. The array had lateral and vertical extents of 2.2 and

0.8 km (1.4 by 0.5 mi), respectively, and essentially surrounded the two longwall panels (figure 2). The underground seismic array consisted of 14 geophones in the mains and bleeders around the longwall panels. The underground geophones were cabled to a central underground computer where the signals were collected and transmitted via fiber-optic network to a main data analysis computer in the mine office (figure 3). On the surface above the mine, 9 geophones were distributed over the panels (figure 2). The signals from the surface network were digitized and transmitted by radio to a digital data acquisition system residing on the same network as the main data analysis computer at the mine office (figure 3). In the data analysis computer, the microseismic event signals were automatically analyzed in order to calculate the event locations, which were then displayed on a computer generated mine map for use by mine personnel. Using this automatic field location process (6), over 13,000 seismic events were detected and located during the mining of panel 2 between December 1999 and May 2000.

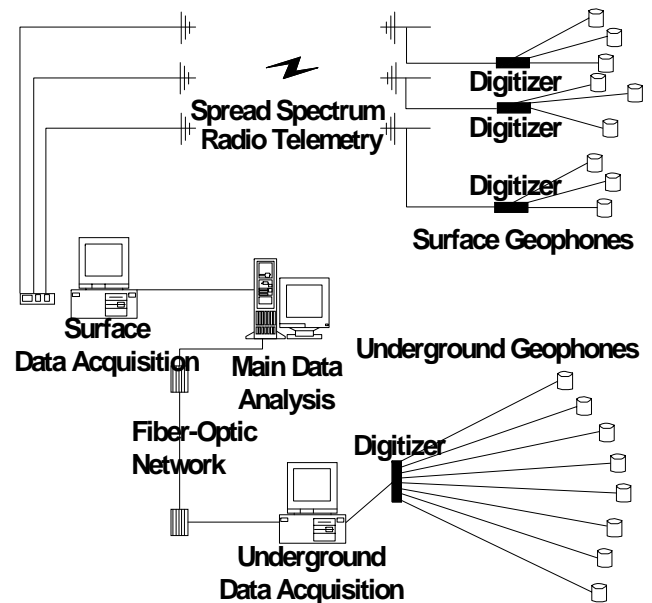


Figure 3. Schematic representation of the microseismic system

MICROSEISMIC DATA PROCESSING

In order to obtain a consistent data set of event locations for this analysis, the raw waveform data were reprocessed in the laboratory. The lab processing utilized an improved seismic velocity model. Seismic velocity data from sonic logs obtained in nearby boreholes were used to create a starting model. Then a number of calibration blasts and other control events with known locations (which were largely at the accessible periphery of the array) were used to further constrain the layered velocity model. This process culminated in a layered seismic velocity model which best fit the available data, although there still appears to be notable spatial variations in the seismic velocity structure that are not considered in the simple uniform layered model. Finally, only the events with a minimum of 8 stations (with at least 3 surface stations and 3 underground stations) reporting good first-arrival picks were kept in the database. This post-processing procedure winnowed the original 13,000 events down to a good quality data set consisting of approximately 5,000 events from panel 2.

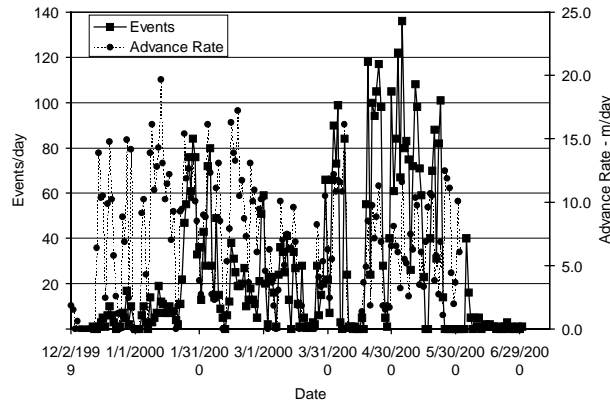


Figure 4. A comparison of the number of events per day with the mining advance rate

EVENT TIMING

One of the first aspects of the seismic data that was investigated in detail was the number and timing of the events. During the six month period that the panel was actively being mined, 5,024 good quality events were recorded. This is an average of 29 events per day with a minimum of 0 and a maximum of 136 events per day. However, the temporal distribution of these events was not very even, as seen in figure 4 and table 1. In the graph in Figure 4, one can see three distinct periods of seismic activity. From the start of the panel on December 2, 1999 until January 20, 2000, when the face had advanced about 300 m (1,000 ft), the seismic activity was fairly low, averaging around 5 events per day. (Also, in general, the events in this time period were relatively smaller (figure 5) and more scattered about the advancing face than in subsequent periods (1)). Then, from January 21 until April 8th, there was a period of intermediate seismic

intensity. This period corresponds to the face moving from 300 to 900 m (1,000 to 3,000 ft) of advance at which point the face was stopped and widened from 165 to 245 m (550 to 820 ft) (figure 2). Within this time period, the activity was relatively higher at the beginning and at the end as the face approached the pillars connecting the adjacent headgate. Also, at several times during this time period the face was stopped and the seismic activity likewise went to zero (figure 4). In the final time period, April 16th to May 24th, when the longwall advanced 300 m (1,000 ft) with the wider face, the seismic activity was quite high averaging 64 events per day.

Table 1. A comparison of the seismic activity between different parts of the panel.

	Advance (m)	Starting Date	Ending date	Total # of events	Average # of events per day
Total Panel	0 - 1200	12/02/99	05/25/00	4,930	29
Early Panel	0 - 300	12/02/99	01/20/00	212	5
Mid Panel	300 - 900	01/21/00	04/08/00	2,232	28
Final Panel	900 - 1200	04/16/00	05/24/00	2,486	64

The next analysis was to correlate the advance rate of the longwall face to the amount of associated seismic activity. Previous research has shown a direct correlation between the mining advance rate and the induced seismicity (9). To perform this analysis, the meters of advance of the longwall face per shift were correlated

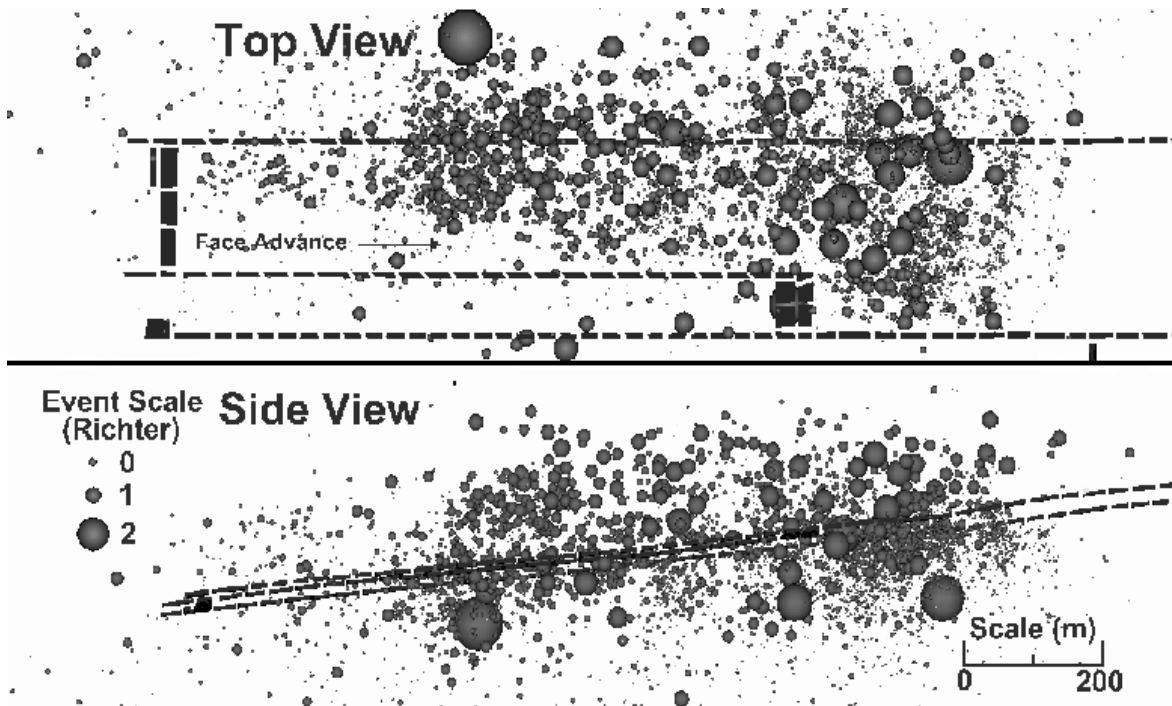


Figure 5. A three-dimensional view of the seismic events with the event size scaled by magnitude (the M_L 4.2 event removed for clarity)

against the number of good quality seismic events that were detected during that shift (and within 4 hours after the face stopped on an idle shift). All of the results of this analysis are shown in table 2 and an example of the linear correlation for the final part of the panel is shown in figure 6. First, looking at the entire panel in table 2, a linear correlation of 2.81 events per meter of advance is determined, but the r^2 value only 25%. However, if the panel is again broken into the same three distinct periods, or section, as above, a much stronger correlation is obtained. In fact, the average r^2 value for the panel divided into the three sections is 58%. This squared value of the correlation coefficient is fairly significant for this type of mining data and signifies that 58% of the fluctuation in the shift-based number of events can be explained by the corresponding fluctuation in the shift

advance rate. Mechanistically, this implies that a majority of the seismic events are a direct result of the advancing face. The same relative intensity of the seismic activity as noted before in the three sections of the panel is, of course, evident in the correlation with advance rate. The first part of the panel averages 0.7 events per meter of advance versus 3.1 events per meter of advance for the middle part of the panel and 8.3 events per meter for the final part of the panel.

Table 2. The results of correlating the seismic activity to the advance rate.

	Advance (m)	Linear Regression ($y = Ax + B$)		
		Events per m (A)	Fixed events per shift (B)	Correlation coefficient ² (r^2)
Total Panel	0 - 1200	2.81	3.87	0.2498
Early Panel	0 - 300	0.70	0.04	0.6681
Mid Panel	300 - 900	3.10	1.92	0.4886
Final Panel	900 - 1200	8.34	7.25	0.5827

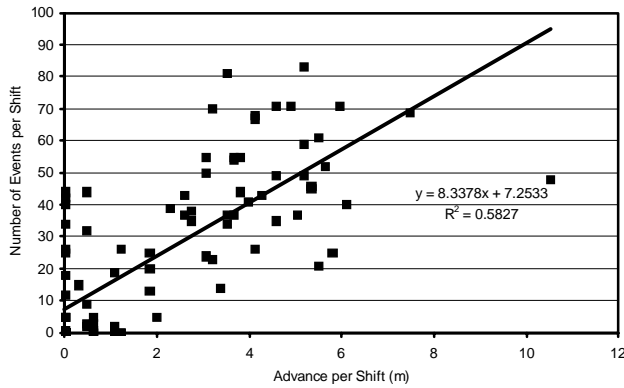


Figure 6. A graph of the correlation between the advance rate and the number of events per shift for the final part of the panel

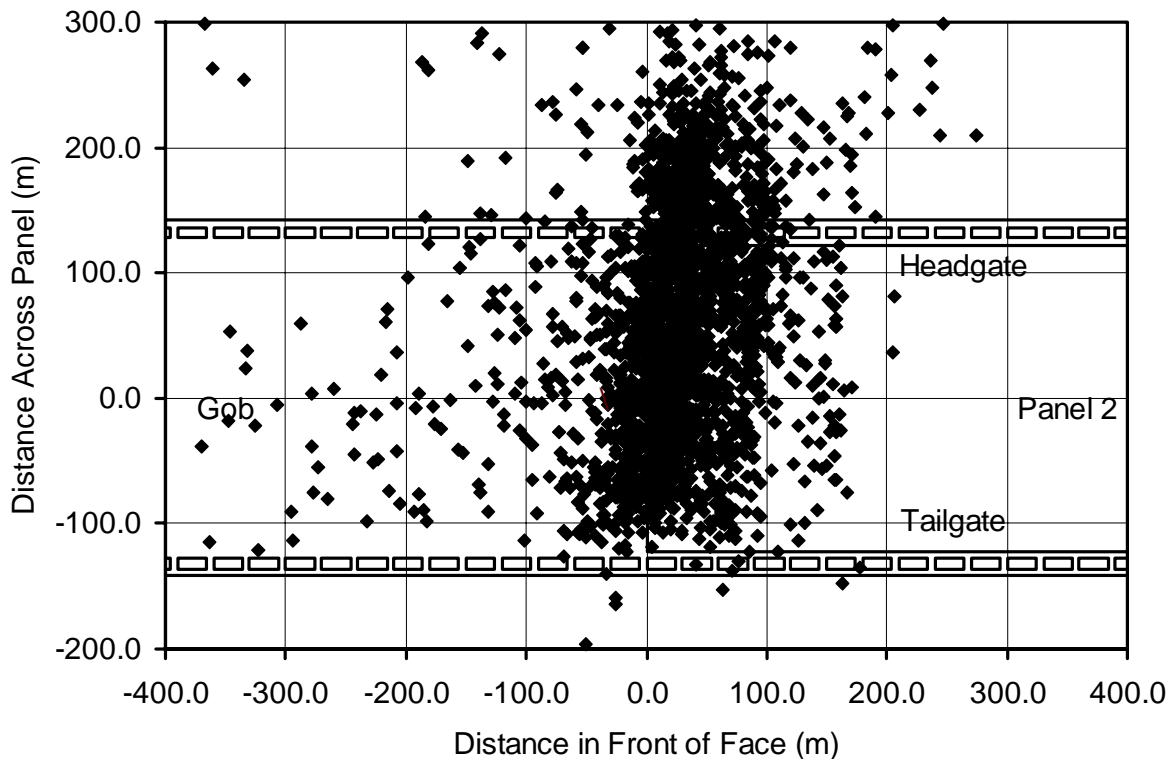


Figure 7. Plan view of the normalized event locations for the last part of panel 2

EVENT LOCATION

Once the optimized velocity model was determined and the final set of good quality seismic events was produced, the location and magnitude of the events were investigated. One of the best means that we found to visualize this “four” dimensional data was to plot the events in three dimensional space as spheres which are scaled by magnitude (figure 5). Taking an overall look at this figure, a number of observations can be made. First, the lack of events in the first 300 m (1,000 ft) of the panel is evident as is the high density of events in the last 300 m (1,000 ft) of the panel. Second, the events appear to be fairly evenly distributed above and below the panel. Third, it appears that there is a higher density of smaller events and an increased frequency of larger events in the last part of the panel as compared to the relatively high percentage of medium size events in the middle part of the panel. Finally, the event locations appear to be horizontally shifted by as much as 75 m (250 ft) toward the headgate and away from the tailgate. This shift is thought to result from deviations of the actual heterogenous, anisotropic, seismic velocity structure from the assumed homogenous, isotropic, layered velocity model. In particular, we know that the geology is highly variable horizontally, and that the previous gob on one side of the panel influences the seismic velocity. So in analyzing the seismic locations, it must be remembered that the overall event locations can be shifted a little horizontally or vertically by a change in the velocity model. However, the final velocity model applied to the data is the best compromise that minimizes the mismatch between calculated event locations and known source locations for a certain number of events. In addition, the relative location and magnitudes of the events are fairly consistent and can be used confidently in making inferences. Development and use of a spatially heterogeneous, time-dependent, three-dimensional seismic velocity model for event locations is beyond the scope of the present work.

In order to visualize the location of the seismic events in relation to the advancing longwall face, the locations of the events were normalized to the face position and plotted on three orthogonal planes such that the center, or zero point, of the normalized coordinate system corresponds to the center of the longwall face at seam level. In this paper, only the events from the last part of the panel will be specifically presented and analyzed using the relative face position since the events at the beginning of the panel provide similar information (1). The results of normalizing the location of the events from the final part of the panel to the face position are shown in plan view in figure 7, in a vertical view parallel to the advance direction in figure 8 and in a vertical view parallel to the longwall face in figure 9.

Figures 7 through 9 indicate that the seismic activity is mostly located in the face area and generally in front of, and below, the face. This agrees with seismic data from other coal mining sites (5) and has been interpreted to represent the failure of the strata in the forward stress abutment zone. It is thought that the rock failures that occur in the confined high stress area in front of the face are well recorded by the seismic system due to the high energy release and good transmission characteristics; however, the low energy, unconfined tension failures of the immediate roof in the gob behind the face are not well recorded because of the low energy release and the high attenuation in this generally broken rock area. From the plan view in figure 7, it can be seen that most of the seismic activity generally lines up in front of the advancing face. There is a little skewness to the event data, with the seismic activity occurring further in front of the headgate than the tailgate. (Also, it can be seen that the events appear shifted towards the headgate. This may be a manifestation of the deviation of the actual velocity structure from that assumed in the model as discussed above.)

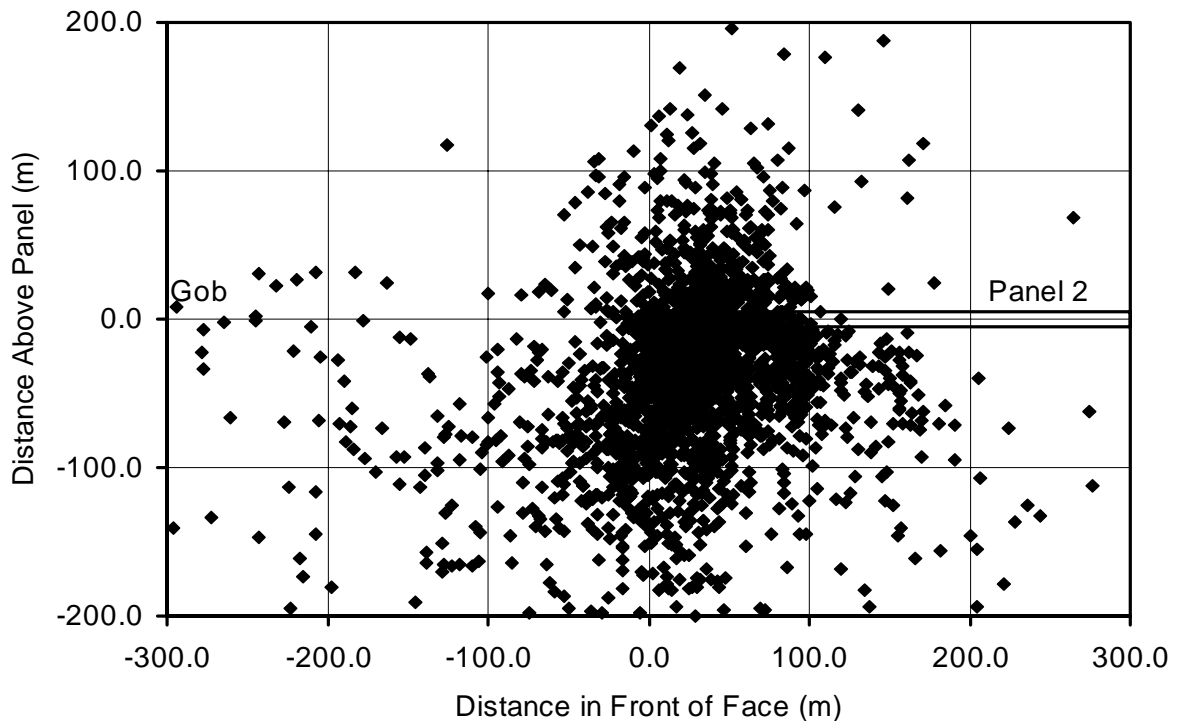


Figure 8. Vertical view parallel to face advance showing the normalized event locations for the last part of Panel 2

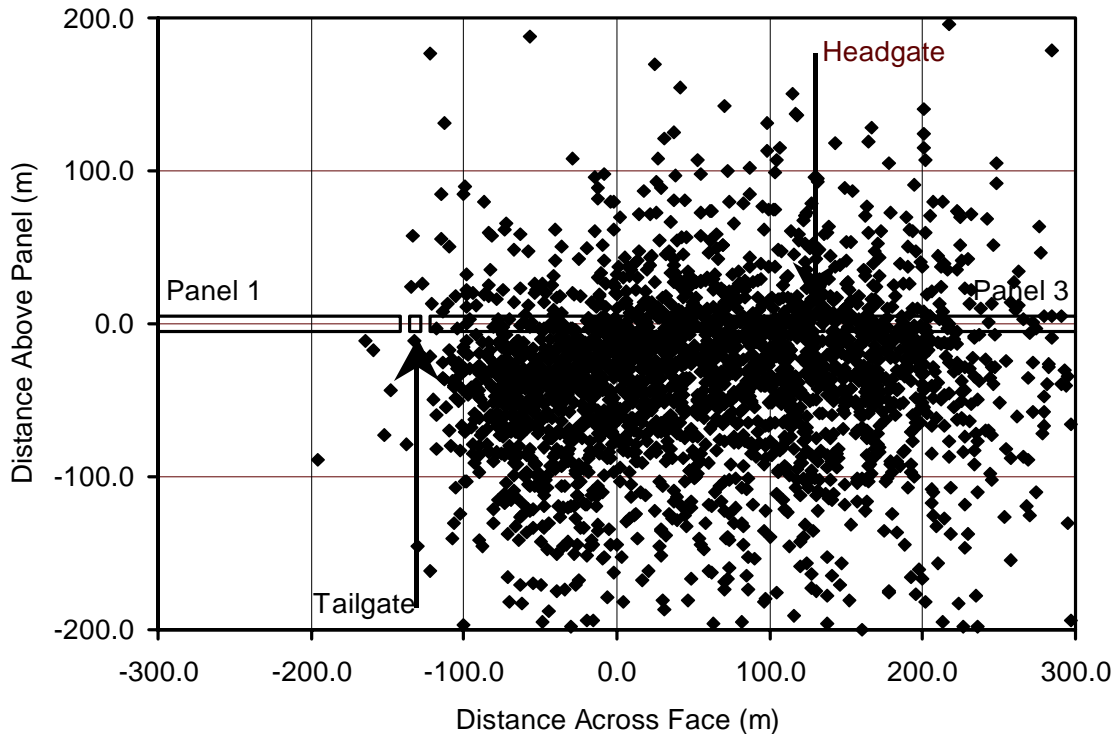


Figure 9. Vertical view parallel to the longwall face showing the normalized event locations for the last part of Panel 2

from the side view in figure 8, it can be seen that the vast majority of the seismic activity is occurring in the face abutment zone, and that there is a notable absence of recorded seismic activity coming from the gob area. Also in Figure 8, it can be seen that the seismicity is originating both above and below the seam level. This response also coincides well with the response observed at other field sites (5) and is consistent with a front abutment stress field that is vertically symmetric about the coal seam. In fact, in figure 8, a majority of the seismic activity appears to be coming from the floor. This response may be due to the presence of more competent floor strata or to a shift of the event locations due to inaccuracies in the assumed velocity model.

MAGNITUDE 4.2 EVENT

On March 6, 2000 at 7:16 pm, MST, a magnitude (M_L) 4.2 “earthquake” occurred in the overburden above the mine and within the confines of the active mine-wide seismic array. The event vibrations were strongly felt by the miners, but there was very little damage from the event on the working longwall face, and only a few rib spalls were evident in the development entries. This is the first time that such an event has been recorded with this detail and accuracy at a U.S. coal mine. This event caused rock slides from critical slopes on the nearby highway, which damaged automobiles. The train tracks adjacent to the highway at that point were also temporarily blocked. Underground, multiple roof falls occurred in the bleeder entries to the west of the first panel and several seals were cracked around the previously abandoned panel. Also, a significant amount of methane was rapidly liberated resulting in a temporary evacuation of the mine. Fortunately, there were no injuries.

Using the optimized velocity model for the site, this event was located 90 m (300 ft) in front of the active face, 170 m (560 ft) above the coal seam and 10 m (35 ft) in from the edge of the 60 m (200 ft) wide barrier pillar between the active and the previous panel (figure 2). This location puts the event near the top of the Blackhawk Formation and the base of the massive Castlegate Sandstone. The event occurred when the active face was approximately 30 m (100 ft) from aligning with the recovery room of the previous panel.

Using P-wave first motion data from the mine wide seismic monitoring system, three temporary University of Utah stations located near the mine and the University of Utah regional seismic network, a well constrained focal mechanism, which fits all of the available P-wave data, was determined. The preferred focal mechanism indicates oblique reverse faulting on a plane dipping steeply to the south or shallowly to the north-northwest (10). The focal mechanism of the event is consistent with the roof strata failing and the Castlegate formation falling into the gob. The location and size of the event and the relative locations of the previous and active longwall faces suggest that the M_L 4.2 event was a failure of the main roof essentially over both panels in the vicinity of the base of the Castlegate. Whether a functional failure of the intervening barrier pillar to fully support the overburden may have preceded and helped initiate the major failure of the main roof is not clear at this time.

CONCLUSIONS

From examining the seismicity at the site, several general observations can be made.

The event rate is low at the beginning of the panel, about six times higher in the middle of the panel, and twice again as high at the wider end of the panel (table 1). We hypothesize that this is a result of the initial gob formation during the beginning part of the panel versus a well established gob through the middle of the panel and then a wider face in the last part of the panel. In fact, when the panel width increased by 50%, we see the seismic activity increase by more than 100%. Also, the correlation between the face advance rate and the seismic activity implies that the majority of the seismicity is a direct and fairly immediate response to removal of the coal and the associated stress redistribution. Looking at the location of the seismic events, it can be observed that the events generally occur in advance of the longwall face and approximately evenly distributed above and below the panel (1). This observation is consistent with the interpretation that the observed seismic events come from failure of the strata in the forward stress abutment zone and is consistent with observation at other sites where the predominant recorded failure mechanism was shear fracture in front of the face as opposed to tensile failure in the gob.

A magnitude 4.2 seismic event occurred within the active longwall panel and was recorded by the mine-wide seismic system giving a unique opportunity to characterize important overburden deformation processes. It has long been acknowledged that not every potentially hazardous bump generates a regional seismic event, nor does every mine-induced, regional seismic event manifest itself as a coal outburst at the seam level. Numerous larger ($> M 2.0$) seismic events have been located near active mines by regional seismic systems (11). Some of these seismic events were associated with coal bumps underground, but many of the larger seismic events caused no observable underground damage. Given the location accuracy of the regional seismic systems, the exact proximity of the seismic event to the coal seam and bump location could not have been determined. Using the mine-wide seismic system in this study, the M_L 4.2 seismic event was relatively accurately located some 150-180 m (500-600 ft) above the longwall face. So at least in this one case, we know that the large seismic event was associated with overburden failure and not with pillar or panel failure. Also, since this very large event was within 180 m of a highly stressed longwall face and there was no noticeable coal discharge, this instance documents a rather dramatic example of how large local seismic events do not necessarily result in face damage. Therefore, this one occurrence suggests that, in order to control coal bumps, mine designers and safety personnel generally need to be more concerned with the seismic events, stress and geologic anomalies that are relatively close (within 30 m (100 ft)) to the working face. Also, the location of this large overburden failure above the intervening "barrier" pillar and the relative closeness of the two longwall faces at the time of the event, suggest that the two longwall gobs were functionally combined at the location of the failure.

In summary, the unique results of this microseismic research project have increased our understanding of the longwall strata failure processes and promise to improve the science of future mine designs.

REFERENCES

1. Ellenberger, J.L., Heasley, K. A., Swanson P.L. and Mercier, J. Three Dimensional Microseismic Monitoring of a Utah Longwall. Proceedings of the 38th U.S. Symposium of Rock Mechanics, Washington DC, July 7-10,2001, in press.
2. Gale, W.J., Heasley, K.A., Iannacchione, A.T., Swanson, P.L., Hatherly, P. and King, .A.. Rock Damage Characterization from Microseismic Monitoring. Proceedings of the 38th U.S. Symposium of Rock Mechanics, Washington DC, July 7-10, 2001, in press.
3. Westman, E.C., Heasley, K.A., Swanson, P. L and Peterson, S. A Correlation Between Seismic Tomography, Seismic Events and Support Pressure. Proceedings of the 38th U.S. Symposium of Rock Mechanics, Washington, DC, July 7-10,2001, in press.
4. Kelly, M., Gale, W.J., Luo, X., Hatherly, P., Balusu R. and LeBlanc, G. Longwall Caving Process in Different Geologic Environments Better Understanding through the Combination of Modern Assessment Methods. Proceedings of the International Conference on Geomechanics/Ground Control in Mining and Underground Construction, Wollongong, NSW Australia, July 14-17, 1998, Vol 2, pp. 573-589.
5. Luo, X., Hatherly, P. and Gladwin, M. Application of Microseismic Monitoring to Longwall Geomechanics and Safety in Australia. Proceedings of the 17th International Conference on Ground Control in Mining, Morgantown, WV, August 4-6 1998, pp. 72-78.
6. Swanson, P.L. Development of an Automated PC-Network-Based Seismic Monitoring System. Proceedings of the 5th International Symposium on Rockbursts and Seismicity in Mines, 2001 In press.
7. Barron, L.R., DeMarco, M. J. and Kneisley, R.O. Longwall Gate Road Stability in Four Deep Western U.S. Coal Mines. USBM IC 9406,1994, 84 pp.
8. Mercier, J. Personal communications with the mine geologist, 2000.
9. Arabasz, W.A., Nava, S.J. and Phelps W.T. Mining Seismicity in the Wasatch Plateau and Book Cliffs Coal Mining Districts, Utah, USA. Proceedings of the 4th International Symposium on Rockbursts and Seismicity in Mines, Krakow, Poland, August 11-14, 1997, pp. 111-116.
10. Swanson, P.L. and Pechmann, J.C.. Focal Mechanism for the March 7, 2000, M 4.2 Willow Creek Earthquake. Personal communication, May 18, 2000.
11. Ellenberger, J.L. and Heasley, K.A. Case Study of Coal Mine Seismicity at the Arch No. 37 Mine, Harlan County, Southeastern Kentucky. NIOSH, Pittsburgh Research Center, Internal Report 4943, 2000, 15 pp.